

# Measurement of Low Concentrations of Nanoparticles in Aerosols Using Optical Dielectric Microcavity: The Case of TiO<sub>2</sub> Nanoparticles

K. N. Min'kov<sup>a, b\*</sup>, A. D. Ivanov<sup>a</sup>, A. A. Samoilenko<sup>a</sup>, D. D. Ruzhitskaya<sup>a, c</sup>,  
G. G. Levin<sup>a</sup>, and A. A. Efimov<sup>d</sup>

<sup>a</sup> All-Russian Research Institute for Optical and Physical Measurements, Moscow, 119361 Russia

<sup>b</sup> Moscow Institute of Electronics and Mathematics, National Research University "Higher School of Economics", Moscow, 123458 Russia

<sup>c</sup> Moscow State University, Moscow, 119991 Russia

<sup>d</sup> Moscow Institute of Physics and Technology, Moscow oblast, Dolgoprudny, 141701 Russia

\*e-mail: kminkov@vniiofi.ru

Received November 10, 2017; accepted for publication February 16, 2018

**Abstract**—A method for measuring low concentrations (up to 0.001 mg/mL) of TiO<sub>2</sub> nanoparticles in aerosols using an optical dielectric microcavity is proposed. The method is based on measuring the change in the microcavity Q factor due to the adsorption of particles on its surface. The results of experimental studies of aerosol samples containing TiO<sub>2</sub> nanoparticles with a diameter of 40 nm with different concentrations are presented. The method for calibrating the measurement channel is developed. The basic requirements for the optical dielectric microcavity as a primary measuring transducer are formulated. The influence of the optical-mode volume on the measurement error is estimated.

DOI: 10.1134/S1995078018010093

## INTRODUCTION

TiO<sub>2</sub> nanoparticles are widely used in various fields of science and technology: in medicine [1], the paint and varnish industry [2], as a catalyst for the oxidation of organic pollutants [3], and in the cosmetic industry [4–6]. Upon penetrating into the human body, nanoparticles can cause harm due to their high biological activity [7, 8]. The probability of receiving a hazardous dose of nanoparticles is particularly high in places where the nanomaterials are produced. Therefore, it is necessary to control the concentration of nanoparticles in the work areas of nanoindustry enterprises. To date, a number of normative documents in the field of hygiene, toxicology, and sanitation regulating requirements for nanomaterials and methods for their control has been adopted in Russia [9–11]. In addition, measurements of the nanoparticle concentration are in high demand in medical studies, where a high sensitivity of measuring instruments is required, and the detection limit can be as low as several nanoparticles [12–14].

The following methods exist to control the concentration of nanoparticles: translucent electron microscopy, static light scattering, counting the condensation nuclei, gravimetric, nephelometric, and piezobalance methods. However, these methods usually use expen-

sive and large equipment or their sensitivity to nano-sized particles is not sufficient.

The need for a compact and inexpensive method for monitoring nanoparticle concentrations in the air of the work area necessitates new alternative measurement methods. The use of an optical dielectric microcavity (ODMC) for measuring the concentration can be such an alternative. The optical radiation in an ODMC propagates in the form of modes, called "whispering gallery" modes. If the ODMC surface has a nanometer roughness at a base length of 10 μm, the optical radiation may experience multiple reflections with very small losses. The Q quality of such a mode can reach a value of 10<sup>11</sup>. The mode field in an ODMC is localized both inside the microcavity and on its surface, allowing the use of the ODMC as a detector of nonuniformity in the environment. The change in the Q factor due to the deposition of particles on the ODMC surface can be measured and used to determine the concentration of nanoparticles (up to single nanoparticles), as well as large molecules [12]. Researchers show significant interest in using the "falling-out" field of the whispering gallery modes for purposes of biodetection in clinical diagnosis [15]. At the moment, descriptions of various test setups for measuring the concentration of single nanoparticles

are available the literature, but, despite this, there are many problems associated with the technical implementation of this method for commercial use. The major part of experimental works describes the measurement of nanoparticle concentration in the liquid medium. This is because their detection in aerosols is a more complex technical task. The calibration of such sensors requires creating an aerosol of nanoparticles with specified parameters, which is a challenging task in itself. There are difficulties in technical implementation, for example, sealing all structural elements, maintaining the distance between the ODMC and the coupling system, and the complexity of cleaning all structural elements.

The aim of this work was to develop and test a prototype sensor on the basis of an ODMC for measuring the concentrations of nanoparticles in aerosols. The sensor was tested using TiO<sub>2</sub> nanoparticles.

This aim required resolving the following tasks: to develop a method for measuring the concentration of nanoparticles and design an experimental setup, to find appropriate methods for dispersing nanoparticles and for calibrating the primary measuring transducer, to analyze the factors affecting the measurement error, and to create a method for reproducing the concentration of TiO<sub>2</sub> aerosol in a limited volume of environment.

### THEORY

The method for measuring the concentrations of nanoparticles is based on the interaction of nanoparticles with an optical radiation field that penetrates into the medium with a lower refractive index at a full internal reflection. This “falling-out” field decays exponentially in the medium. Nanoparticles adsorbed on the microcavity surface are in the range of action of the falling-out field, which interacts with any optical inhomogeneities located on the surface of the microcavity near its equatorial part, where the whispering gallery mode is localized. As a consequence, the frequency characteristics of the ODMC, which that can be used to evaluate the concentration and size of the nanoparticles [16]. With the help of this method, it is also possible to estimate the nanoparticle mass if the polarizability of a separate nanoparticle is known [17]. There are several mechanisms that influence on the spectrum of the resonance mode ODMC:

- (1) shift of the resonance frequency due to an increase in the optical-path length in the resonator [18];
- (2) splitting of the mode due to the reflection of scattered light back into the cavity and the formation of a counterpropagating wave [19];
- (3) broadening of the mode caused by energy losses due to the scattering on optical inhomogeneities [20].

It should be noted that all these mechanisms can manifest themselves simultaneously [21].

Among the above, the mode broadening mechanism is most sensitive and allows measuring the concentration of particles with a size up to 10 nm [22] when using microcavities with a Q factor of 10<sup>8</sup> [20]; in addition, this mechanism is insensitive to temperature fluctuations. For this reason, the sensor prototype tested in this work was based on this method.

The concentration of nanoparticles in the air is calculated from the Q-factor change rate using calibration characteristics for a particular type of ODMC and the known size and type of nanoparticles. Considering the dependence of the resonance peak width on the time during which the particles settle on the ODMC surface, one can note that its initial part, when the particles settle on the free adsorption centers, is linear. The probability of “sticking” to the ODMC surface reduces in time as the adsorption centers become partially filled. After some time, the dependence reaches saturation. Thus, the derivative taken at the initial part of this Q-factor degradation curve yields a tangent slope which is proportional to the concentration of nanoparticles.

### EXPERIMENTAL

An experimental setup was developed to realize the above-described measuring technique. The optical part of the sensor is described in [23]. The whispering gallery modes were excited using a tunable VitaWave ECDL6707R laser. The central wavelength of the laser was 670 nm and the tuning range was about 15 GHz. The ODMC was located in a sealed flow cell. A triangular prism or a stretched optical fiber was used as a coupling element with the microcavity [24]. The prism is more difficult in alignment, but it is more resistant to external vibrations. Stable coupling requires maintaining the gap on the order of the exciting radiation wavelength between the ODMC surface and the coupling element. For this reason, the design of the measuring cell used the prism as the coupling element. The ODMC was positioned relative to the coupling element with the use of a piezo motor. The radiation passing through the ODMC was recorded using a photodetector. The photodetector signal was processed by an oscilloscope.

The first experimental task was to calibrate the primary measuring transducer, which was the ODMC. This required a flow of the aerosol of TiO<sub>2</sub> nanoparticles with a known concentration. For this purpose, TiO<sub>2</sub> nanopowder obtained by the electric explosion of wire (EEW) was used [25]. The EEW nanopowder was obtained by fast (microsecond) heating and the electric explosion of a segment of titanium wire upon applying a pulse of high-density electric current, 10<sup>4</sup>–10<sup>6</sup> A/mm<sup>2</sup>, in a mixture of inert gas with oxygen. The EEW process forms a high-density vapor-drip mixture which rapidly expands into the surrounding gas. This leads to a sharp decrease in the vapor concentration

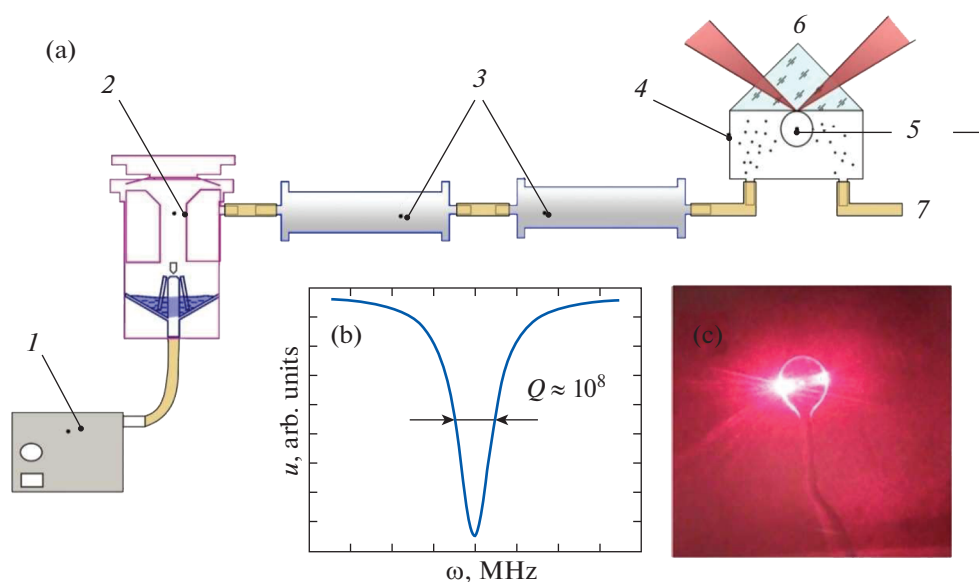


**Fig. 1.** (Color online) (a) Scheme of the system for dispersing titanium dioxide nanoparticles in air: (1) compressor, (2) nebulizer, (3) dehumidifiers with zeolite, (4) cell, (5) ODMC, (6) optical coupling system, and (7) hood. (b) Resonance curve with a  $Q$  factor of  $Q = 10^8$ . (c) An ODMC with an excited whispering gallery mode.

(temperature) and its condensation with the formation of nanoparticles.

The experimental setup, which was designed for the calibration of the ODMC, is described in detail in [26]. The drawback of this setup was the lack of reproducibility of the experimental results. This drawback was eliminated by replacing the aerosol delivery system.

The modernized dispersion system is shown in Fig. 1. This system works as follows: compressor 1 supplies compressed air at a speed of 2 to nebulizer flask 2, which is filled with hydrosol. Because the tube diameter decreases toward the nebulizer inlet, the pressure of the compressed air drops and, as a consequence, the speed of the compressed air flow increases. The solution with particles is sucked from the flask into the area of reduced pressure [27]. As a result, at the output, one obtains an aerosol saturated with  $\text{TiO}_2$ . When it passes through dehumidifiers 3, water evaporates and the aerosol consisting of  $\text{TiO}_2$  nanoparticles enters cell 4. Dehumidifiers are hollow cylinders with a central unit made of a netting material along the axial line. The space between the walls of the dryer and the central unit is filled with zeolite. In cell 4, the particles are adsorbed on the surface of replaceable microcavity 5. Prism 6 provides both the input and output of light from the microcavity. Particles that were not adsorbed enter hood 7.

The  $\text{TiO}_2$  nanoparticle hydrosol was prepared in three mass concentrations: 1, 0.03, and 0.001 mg/mL according to the method described in [28].

The measurement of the concentration using an ODMC consisted of the following steps. In the first step, an ODMC was placed in the cell; then the cell was sealed and connected to the dispersion system. After that, an optical connection with ODMC was established by setting the gap between the prism and the ODMC, first using a rough mechanical driver and then a fine piezo-driver. This is accompanied by the appearance of an inverted resonance peak on the oscilloscope screen. The next step was to determine the  $Q$  factor of the ODMC [20], which should not be less than  $10^6$ . Next, with the help of the dispersion system presented in Fig. 1, the aerosol was fed into the cell, with the constant component of the laser tuning being adjusted in such a way that the resonant peak remained within the range of the oscilloscope sweep. The signal was recorded for 600 s. After that, the ODMC microsphere with a thin film of nanoparticles on its surface was photographed.

The oscilloscope signal was processed as follows. First, a sequence of microcavity transmission spectra was recorded. These spectra exhibited resonance curves of the work mode of the whispering gallery in the form of inverted peaks. Next, this sequence of the resonator spectra was processed, including the subtraction of the resonance peak drift and normalization. Then the peak width versus time was calculated. The resulting dependence was filtered to remove the noise. Next, the slope of the linear part of the resulting curve was determined, which is equal to the broadening rate of the resonator work mode. The broadening rate was proportional to the rate of particle deposition on the microcavity surface.

**Table 1.** Results of nanoparticle measurement by the method of differential electric mobility

Mass concentration of hydrosol (mg/mL)	0.001	0.03	1
Integral counted concentration of the aerosol, $10^5$ particles/cm <sup>3</sup>	$1.55 \pm 0.12$	$2.92 \pm 0.19$	$7.95 \pm 0.21$

To calibrate the ODMC, the concentration of nanoparticles in the volume of the cell should be estimated. Initially it was planned that the concentration of TiO<sub>2</sub> nanoparticles in the aerosol would be controlled using a KANOMAX 3521 aerosol analyzer. This model uses the piezobalance measurement method [29, 30], which is based on charging the aerosol particles in the field of a corona discharge. The charged particles settle on the surface of the quartz piezoelectric element, which leads to a change in the oscillation frequency of the quartz crystal. However, the presence of particles in the air stream was not revealed, because this device is insensitive to particles smaller than 100 nm.

In this regard, the concentration was determined by the method of differential electric mobility of aerosol particles using a TSI SMPS 3936 (TSI Inc., United States) aerosol spectrometer. The method is based on the separation of aerosol particles by size as they pass through the electric field [31], where the charged aerosol particles change their trajectory depending on their size, the aerosol flow rate, and the strength of the electric field. This method revealed the dependence presented in Table 1. These data are consistent with the results of our experiment.

The size of titanium dioxide particles obtained by the EEW method was determined using transmission electron microscopy. The primary particle size was determined on a JEOL JEM-2100 transmission elec-

tron microscope with an accelerating voltage of 120 keV. The measurement results showed that the effective size of the identified particles varies from 3 to 35 nm. The appearance of titanium dioxide particles is shown in Fig. 2a.

The size of nanoparticles in the cell volume was measured by the deposition of particles on a control spot (target) with the use of electron microscopy. To do this, the air flow, which contains TiO<sub>2</sub> nanoparticles and is directed from the top on the target with a sticky layer, was closed for 1 s. The image of nanoparticles on the target was obtained at a hydrosol concentration of 0.001 mg/mL using a Nvision 40 scanning electron microscope and an Inlens detector. The density of particles was calculated with the help of a raster electron microscope in three areas 1 mm<sup>2</sup> in size; the obtained average value was 32 particle/mm<sup>2</sup> (for a hydrosol concentration of 0.001 mg/mL). Thus, these experiments gave an idea of the shape and size of the particles which enter the cell and settle on the ODMC surface. The appearance of TiO<sub>2</sub> nanoparticles on the surface of conductive adhesive tape is shown in Fig. 2b.

## EXPERIMENTAL RESULTS

The calibration at a constant concentration revealed that, despite the fact that the concentration in the aerosol was stable for each series of measurements,

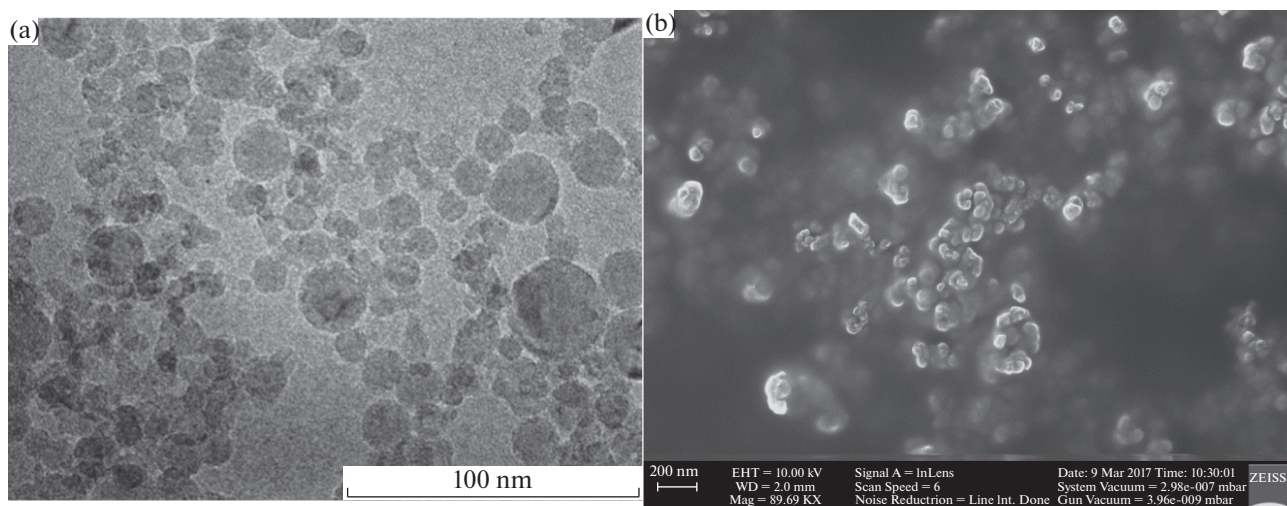


**Fig. 2.** Photos of titanium dioxide particles: (a) photograph of titanium dioxide particles of the primary size obtained using a JEOLJEM-2100 transmission electron microscope at an accelerating voltage of 120 keV; (b) photograph of particles adsorbed on the surface of a conductive adhesive tape obtained using a Nvision40 raster electron microscope at an accelerating voltage of 10 keV and an Inlens detector.

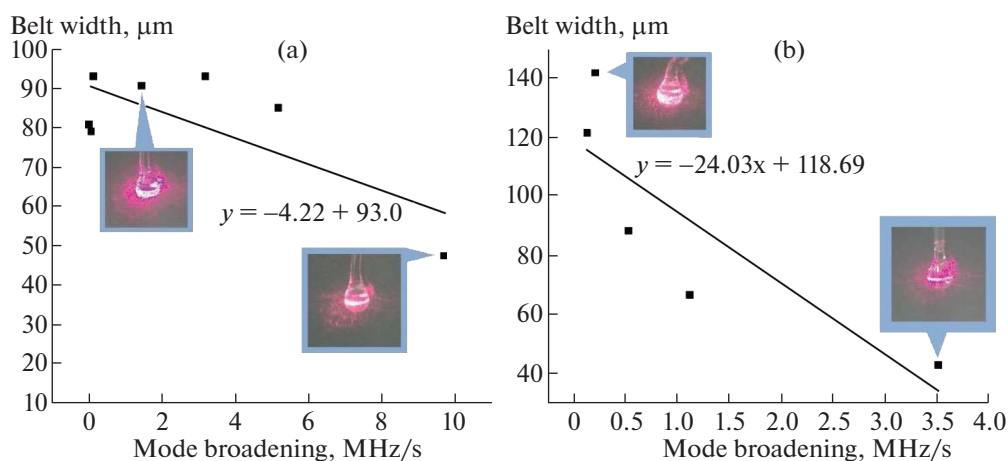


**Fig. 3.** (Color online) Dependence of the belt width on the rate of mode broadening at a concentration of (a) 0.001 mg/mL and (b) 0.03 mg/mL, respectively.

the resonance degradation rate varied significantly (up to two orders).

One reason for this variation may be the dependence of the sensitivity on the mode volume, i.e., the volume occupied by the whispering gallery mode in the resonator. The fact is that the contribution of an individual particle adsorbed on the ODMC surface to the resonance curve broadening depends on the degree of spatial localization of the mode field. A mode of a low spatial order has a small volume, and each particle interacts with a significant fraction of the radiation energy accumulated in the mode. The volume occupied by a high-order mode is larger and the fraction of energy in the mode per each particle is smaller. The mode volume depends on the ODMC geometry and varies for each sample.

The width of the luminous “belt,” which can be observed with a microscope on the ODMC surface when particles are adsorbed on it, was used as a diagnostic parameter for estimating the volume occupied by the radiation in the mode. For this reason, the ODMC was photographed after each experiment. An example of such a micrograph is shown in Fig. 1d (Figure absent). Also, the mode volume was directly influenced by the microsphere diameter, which was controlled by a Leica DCM 3D microscope and amounted to  $300 \pm 10 \mu\text{m}$ . Thus, for modes with a wide belt, the contribution of each particle to the resonance curve broadening should be less than for modes with a narrow belt. At the same rate of particle deposition on the microcavity surface, the rate of resonance curve broadening should change accordingly.

Figure 3 shows the results of experiments on determining the dependence of the mode broadening rate on the belt width. As is seen, the variation of the measured values is significant, with the mean square deviation (MSD) being about 40% of the broadening rate value. The results were approximated by a linear

dependence. In the case of a narrow mode distribution, the sensitivity exhibits a significant increase.

Still, at the same concentration of particles, the scattering of measurement results decreases 2.5 times after correcting the data according to expression 1, which is associated with the ODMC mode volume,

$$\Delta\omega' = \Delta\omega - X + \Delta\omega_{cp}, \quad (1)$$

where  $\Delta\omega'$  is the corrected value of mode broadening,  $\Delta\omega$  is the value without correction,  $X$  is the value of the correction in accordance with the linear dependence on the mode volume, and  $\Delta\omega_{cp}$  is the arithmetic mean over the measurement results at the same concentration.

These results lead to a number of requirements for the ODMC as a measuring transducer of a highly sensitive sensor:

- the calibration of the microcavity should include a procedure for controlling the mode volume and diameter of the microsphere;
- a wide belt and, accordingly, a high mode index indicate that the given microcavity has defects;
- due to the high sensitivity of the sensor, the microcavity should be placed in a clean, sealed container immediately after their production;
- for this method, the low detection limit is reached for microcavities with a Q factor of  $10^6$  and above [20].

## DISCUSSION

Thus, this method is capable of measuring concentrations of  $\text{TiO}_2$  nanoparticles in aerosols at low concentrations down to 0.001 mg/mL. The method was tested using a setup for dispersing the nanoparticles, with the dispersion characteristics being measured by methods of differential electrical mobility and transmission electron microscopy. The accuracy of con-

centration measurements with the use of an ODMC significantly depends on the calibration of the measuring channel and the microsphere manufacturing quality. In addition to the influence of the mode volume, another reason for the scattering of measurement results can be the static charge on the ODMC surface, the value of which can significantly affect its adsorption capacity. Controlling the surface charge is a complex experimental task and was not considered in this work. In addition, it is also possible that the particles coagulate, forming agglomerates. The influence of aerodynamic forces and dynamic adsorption characteristics are subjected to significant changes as the particle size increases. The coagulation rate increases in turbulent flows and fine particles are strongly affected by small changes in the air flow rate, which in turn can lead to a change in the deposition rate and an error in determining the mass concentration.

The volume of the resonator mode determines the active area of interaction and, as a consequence, affects sensor sensitivity. The method of controlling the mode volume of each ODMC has an error associated with determining the microsphere diameter and the size of the luminous area occupied by the field of the whispering gallery mode.

Further improving the accuracy of this method requires studying the reproducibility of the adsorption properties of the ODMC surface and experiments with selective adsorption coatings for other types of nanoparticles.

Still, the sensing element of the measuring channel is small, and the optical signal can be commutated using an optical fiber. Quartz spheres as single-use sensitive elements can be obtained by heating rods of high purity quartz. The fabrication of these microcavities is straightforward. The most expensive element of such a sensor is the tunable laser. For this reason, it is advisable to build a multichannel measurement system and use one laser for several measuring cells. In this case, a highly sensitive sensor of aerosol nanoparticles can be created on the basis of this method, the sensing element of which can be positioned at a significant distance from the measuring equipment.

## CONCLUSIONS

The possibility of detecting small concentrations of nanoparticles in the air with the help of a spherical optical microcavity was experimentally confirmed using TiO<sub>2</sub> nanoparticles as an example for demonstration. A prototype of a highly sensitive sensor was built and tested. A method of dispersing TiO<sub>2</sub> nanoparticles to calibrate the ODMC sensor was developed.

It was shown that introducing a correction of the ODMC mode volume eliminates the systematic component of the measurement error associated with the variation in the active area of interaction. After the

correction, the mean square deviation of measurement results at the same concentration amounts to 15%.

One prospective direction for developing this method is the application of selective coatings on the ODMCR surface, which allow the selection of separate elements from the substance. Currently, such coatings are used for biological objects in medical diagnostics [31]. In the present work the ODMC was used without selective coatings, but these prototype measuring transducers are able to register the presence of nanoparticles in the air of clean rooms or in the work area of nanoindustry enterprises.

Owing to their ability to detect concentrations down to single particles, the ODMC sensors can be considered a basis for future instruments.

## ACKNOWLEDGMENTS

This work was performed using equipment from the center for collective use of high-precision measurement technologies in the field of photonics at the All-Russian Research Institute for Optical and Physical Measurements (ckp.vniiofi.ru). The work was supported by a grant from the president of the Russian Federation for state support of young Russian scientists, MK-2302.2017.8.

## REFERENCES

1. P. C. Maness, S. Smolinski, D. M. Blake, Z. Huang, E. J. Wolfrum, and W. A. Jacoby, "Bactericidal activity of photocatalytic TiO<sub>2</sub> reaction: toward an understanding of its killing mechanism," *Appl. Environ. Microbiol.* **65**, 4094–4098 (1999).
2. J. H. Braun, A. Baidins, and R. E. Marganski, "TiO<sub>2</sub> pigment technology: a review," *Prog. Org. Coat.* **20**, 105–138 (1992).
3. J. Jin, S. G. Kwon, T. Yu, M. Cho, J. Lee, J. Yoon, and T. Hyeon, "Large-scale synthesis of TiO<sub>2</sub> nanorods via nonhydrolytic sol-gel ester elimination reaction and their application to photocatalytic inactivation of *E. coli*," *J. Phys. Chem.* **109**, 15297–15302 (2005).
4. X. Chen and S. S. Mao, "Titanium dioxide nanomaterials: synthesis, properties, modifications, and applications," *Chem. Rev.* **107**, 2891–2959 (2007).
5. L. C. Renwick, D. Brown, A. Clouter, and K. Donaldson, "Increased inflammation and altered macrophage chemotactic responses caused by two ultrafine particle types," *Occup. Environ. Med.* **61**, 442–447 (2004).
6. A. P. Popov, A. V. Priezzhev, J. Lademann, and R. Myllylä, "TiO<sub>2</sub> nanoparticles as an effective UV-B radiation skin-protective compound in sunscreens," *J. Phys. D: Appl. Phys.* **38**, 2564–2570 (2005).
7. J. R. Gurr, A. S. Wang, C. H. Chen, and K. Y. Jan, "Ultrafine titanium dioxide particles in the absence of photoactivation can induce oxidative damage to human bronchial epithelial cells," *Toxicology* **213**, 66–73 (2005).

8. N. Serpone, D. Dondi, and A. Albini, "Inorganic and organic UV filters: their role and efficacy in sunscreens and sun care products," *Inorg. Chim. Acta* **360**, 794–802 (2007).
9. GOST (State Standard) No. R 55723-2013: "Nanotechnologies. Guide to determining the characteristics of industrial nanoobjects" (2014).
10. MR (Guidelines) no. 1.2.2522-09: "Identification of nanomaterials posing a potential hazard to human health" (2009).
11. MR (Guidelines) No. 1.2.0043-11: "Control of nanomaterials in environmental objects" (2011).
12. K. D. Heylman, K. A. Knapper, and R. H. Goldsmith, "Photothermal microscopy of nonluminescent single particles enabled by optical microresonators," *J. Phys. Chem. Lett.* **5**, 1917–1923 (2014).
13. P. Zijlstra, P. M. R. Paulo, and M. Orrit, "Optical detection of single non-absorbing molecules using the surface plasmon resonance of a gold nanorod," *Nat. Nanotechnol.* **7**, 379–382 (2012).
14. T. P. Burg, M. Godin, S. M. Knudsen, W. Shen, G. Carlson, J. S. Foster, K. Babcock, and S. R. Manalis, "Weighing of biomolecules, single cells and single nanoparticles in fluid," *Nature (London, U.K.)* **446**, 1066–1069 (2007).
15. G. C. Righini and S. Soria, "Biosensing by WGM microspherical resonators," *Sensors* **905**, 905 (2016).
16. F. Vollmer and L. Yang, "Label-free detection with high-q microcavities: a review of biosensing mechanisms for integrated devices," *Nanophotonics*, No. 1, 267–291 (2012).
17. F. Vollmer, S. Arnold, and D. Keng, "Single virus detection from the reactive shift of a whispering-gallery mode," *Proc. Natl. Acad. Sci. U. S. A.* **105**, 20701–20704 (2008).
18. F. Vollmer, I. Teraoka, and S. Arnold, "Perturbation approach to resonance shifts of whispering-gallery modes in a dielectric microsphere as a probe of a surrounding medium," *J. Opt. Soc. Am.* **20**, 1937–1946 (2003).
19. S. K. Ozdemir, J. Zhu, L. He, and L. Yang, "Estimation of Purcell factor from mode-splitting spectra in an optical microcavity," *Phys. Rev. A* **83** (3), 5 (2011).
20. Y. Hu, L. Shao, S. Arnold, Y.-C. Liu, C.-Y. Ma, and Y.-F. Xiao, "Mode broadening induced by nanoparticles in an optical whispering-gallery microcavity," *Phys. Rev. A* **90**, 10 (2014).
21. W. Kim, S. K. Özdemir, J. Zhu, L. Hee, and L. Yang, "Demonstration of mode splitting in an optical microcavity in aqueous environment," *Appl. Phys. Lett.* **97**, 071111 (2010).
22. M. R. Foreman, J. D. Swaim, and F. Vollmer, "Whispering gallery mode sensors," *Adv. Opt. Photon.* **7**, 168–240 (2015).
23. A. A. Samoilenko, G. G. Levin, V. L. Lyaskovskii, K. N. Min'kov, A. D. Ivanov, and I. A. Bilenko, "Application of whispering-gallery-mode optical microcavities for detection of silver nanoparticles in an aqueous medium," *Opt. Spectrosc.* **122**, 1002 (2017).
24. A. D. Ivanov, K. N. Min'kov, and A. A. Samoilenko, "Method of producing tapered optical fiber," *J. Opt. Technol.* **84**, 500–503 (2017).
25. Yu. A. Kotov, "The electrical explosion of wire: a method for the synthesis of weakly aggregated nanopowders," *Nanotechnol. Russ.* **4**, 415–424 (2009).
26. Yu. M. Zolotarevskii, K. N. Min'kov, A. D. Ivanov, and A. A. Samoilenko, "Experimental researches of titanium dioxide nanoparticles detection possibility in air medium by means of optical resonators," in *Proceedings of the Conference on Applied Optics, St. Petersburg, 2016*, p. 3.
27. M. F. Muers, "Overview of nebulizer treatment," *Thorax* **52**, 25–30 (1997).
28. A. A. Lizunova, E. G. Kalinina, I. V. Beketov, and V. V. Ivanov, "Development of reference materials for the diameter of nanoparticles of colloidal solutions of aluminum oxide and titanium dioxide," *Meas. Tech.* **57**, 848–854 (2014).
29. GOST (State Standard) No. R 8.791-2013: "Radioisotope and piezo-balanced measuring instruments of mass concentration of dust in the air working area. Verification procedure" (2013).
30. X. Zhang, L. Liu, and L. Xu, "Ultralow sensing limit in optofluidic micro-bottle resonator biosensor by self-referenced differential-mode detection scheme," *Appl. Phys. Lett.* **104**, 033703 (2014).
31. GOST (State Standard) No. R 8.775-2011: "Disperse composition of gaseous media. determination of nanoparticle sizes by the method of differential electric mobility of aerosol particles" (2011).

*Translated by V. Alekseev*

SPELL: OK